ISSN 0027-1349, Moscow University Physics Bulletin, 2014, Vol. 69, No. 1, pp. 37–46. © Allerton Press, Inc., 2014.
Original Russian Text © B.S. Ishkhanov, I.M. Kapitonov, A.A. Kuznetsov, V.N. Orlin, H.D. Yoon, 2014, published in Vestnik Moskovskogo Universiteta. Fizika, 2014, No. 1, pp. 35–43.

Photodisintegration of Molybdenum Isotopes

B. S. Ishkhanov[a, b], I. M. Kapitonov[a], A. A. Kuznetsov[b], V. N. Orlin[b], and H. D. Yoon[a]

[a] *Department of Physics, Moscow State University, Moscow, 119991 Russia*
[b] *Skobel'tsyn Institute of Nuclear Physics, Moscow State University, Moscow, 119991 Russia*
e-mail: gluecklich81@gmail.com

Received October 11, 2013; in final form, October 22, 2013

Abstract—The process of photodisintegration of molybdenum isotopes was studied using the induced activity method. The yields of isotopes produced as a result of photonuclear reactions on a natural mixture of molybdenum isotopes were determined at an electron accelerator energy of 67.7 MeV. A comparison of the experimental results with the theoretical calculation carried out using the combined model of photonucleon reactions shows that the model gives a fair description of the experimental yields of photonucleon reactions on all molybdenum isotopes except for ^{92}Mo. The high yields of the proton channels of photonuclear reactions on the ^{92}Mo isotope and low yields of the corresponding neutron channels are interpreted based on the shell structure of molybdenum isotopes.

Keywords: photonuclear reaction, photodisintegration, molybdenum.

DOI: 10.3103/S002713491401007X

INTRODUCTION

The method of sounding atomic nuclei with a high-energy photon beam is one of the most important methods of their study. If the photon energy reaches several tens of megaelectronvolts, collective oscillations of nucleons of various types are vigorously excited within the nuclei. Such oscillations are classified according to the angular momentum, parity, and isospin quantum number. Isovector electric dipole (E1) oscillations called the giant dipole resonance (GDR) are the dominant mode of collective oscillations in the photon energy range of 10–35 MeV. The study of this phenomenon revealed its fundamental importance for the understanding of dynamics of high-energy nuclear excitations [1–4].

Giant dipole resonance predominantly decays with the ejection of nucleons. The decays with the ejection of a single nucleon (a neutron or a proton) from a nucleus (i.e., reactions (γ, n) and (γ, p)) are prevalent in the region of the GDR maximum (13–25 MeV) and below. It is these reactions in which the nucleus is excited by photons of the bremsstrahlung or quasimonochromatic radiation and the nucleons are detected via direct methods that were used earlier in the vast majority of experiments concerned with the study of GDR [4]. However, the methods of direct detection of nucleons are of little use when the photon energy reaches the GDR maximum or exceeds it. Photonucleon reactions with the ejection of two, three, or more nucleons from the excited nucleus are prevalent in the photodisintegration of nuclei in the energy region $E >$ 25 MeV, and the methods of direct detection of nucleons do not allow one to reliably differentiate reactions of unlike types. For example, it is a rather standard situation when a high-energy photon initiates the photodisintegration of a nucleus and the sole detected neutron may not be decisively attributed to one of the following reactions: (γ, n), (γ, np), or (γ, $n2p$). The same is true when a single proton is detected in reactions (γ, p), (γ, np), and (γ, $2np$). An even more complex situation arises when more than one neutron is emitted from the nucleus. This problem is especially acute in the studies of photonucleon reactions on medium and heavy nuclei mostly accompanied by neutron emission. The lack of reliable data on different nuclei photodisintegration channels precludes one from drawing conclusions on the mechanism of GDR decay in medium and heavy nuclei and on the role that the processes in the high-energy region of the nuclear photodisintegration cross section (such as the quadrupole and quasideuteron photodisintegration) play.

The present work is aimed at studying the photodisintegration of molybdenum isotopes in the region of photon energies extending up to 67.7 MeV experimentally and theoretically. The experiments were conducted for stable molybdenum isotopes (^{92,94,95,96,97,98,100}Mo). The theoretical calculations were carried out for all (including the unstable ones) molybdenum isotopes with mass numbers ranging from 89 to 103. The combined model of photonucleon reactions (CMPR) was used [5].

Several earlier papers [6–9] addressed the issue of photodisintegration of molybdenum isotopes in the GDR region. The authors of [6] determined the cross section of the ^{92}Mo(γ, n)^{91}Mo reaction with a bremsstrahlung beam. The induced activity of the

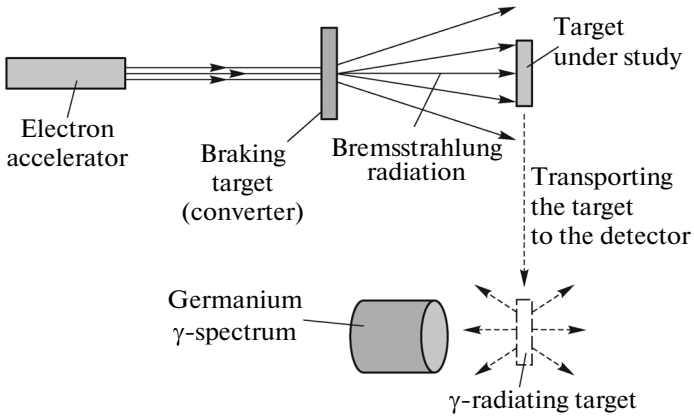

Fig. 1. Scheme of the photonuclear γ-activation experiment.

^{91}Mo nucleus was used. The cross section was measured up to an energy of 23.6 MeV. The authors of [7] determined the cross sections of the $(\gamma, n) + (\gamma, pn) + 2(\gamma, 2n)$ reaction for two molybdenum isotopes (^{92}Mo and ^{98}Mo) with a bremsstrahlung beam using the method of direct detection of photoneutrons. The cross sections were determined up to an energy of 30 MeV. An intermediate structure was observed in the cross-sections. The cross sections of photoneutron reactions on five stable molybdenum isotopes (^{92,94,96,98,100}Mo) were determined in [8]. A beam of quasimonochromatic annihilation photons and the direct neutron detection method were used. The maximum photon energy equaled 26.8–29.5 MeV. The cross section of $(\gamma, n) + (\gamma, pn)$, $(\gamma, 2n)$, and $(\gamma, 3n)$ reactions were obtained. The data on ^{92}Mo and ^{98}Mo isotopes presented in [7] and [8] broadly agree with each other. The photoproton GDR decay channel of the ^{92}Mo isotope was studied in a $(e, e'p)$ experiment [9]. Using the virtual photons technique, the authors of this paper measured the cross section of the $(\gamma, p) + (\gamma, pn) + 2(\gamma, 2p)$ reaction up to an energy of excitation of the target nucleus of 25.4 MeV. The authors of [10] analyzed the available experimental data and determined the estimated photoabsorption cross section for the ^{92}Mo nucleus up to an excitation energy of 25.2 MeV.

The experimental studies reported in the present paper were conducted using the induced gamma-activity method that, contrary to the methods of direct detection of reaction products, allows one to unambiguously isolate photonucleon reactions of different types. The target in such studies is irradiated with a bremsstrahlung γ-beam of the accelerator and is then transported to a γ-spectrometer that measures the γ-spectra of the residual β-activity outside the beam (Fig. 1). A single experiment of this type allows one to gather the data on all photonucleon reactions on all isotopes in the target and gain an understanding of the influence exerted by the ratio of neutron and proton numbers in the nucleus on the competition between different channels of its photodisintegration. The fact that the measurements are conducted outside the beam helps to reduce the background, increases the experimental sensitivity manyfold, and helps one to study the channels of atomic nuclei photodisintegration with low reaction cross sections that earlier were inaccessible to observation. Compared to the methods of direct detection of photonuclear reaction products, the induced activity method requires less complex measurement setups and, if the radioactive nuclei have long half lives, allows one to conduct repeated measurements in order to gather the maximum possible amount of data on the partial reaction channels. The end result of the induced-activity method consists in determining the yield of radioactive nuclei produced in a target irradiated with gamma quanta.

The efficient application of this research technique is promoted by the availability of intense electron accelerators up to the energies of several tens of megaelectronvolts, the use of efficient high-resolution γ-spectrometers with ultrapure germanium, and the availability of extensive and reliable data on the schemes of the residual activity levels and the properties of nuclei that are organized in international nuclear databases [11].

1. EXPERIMENTAL TECHNIQUE

The experiment was carried out using the bremsstrahlung beam of a pulsed sectional microtron RTM-70 with a maximum electron energy of 67.7 MeV installed in the Skobel'tsyn Institute of Nuclear Physics [12]. Its main elements are the linear accelerator and the deflecting magnets ensuring that the electron beam recirculates 14 times. Precision deflecting magnets based on a rare-earth permanent Sm–Co magnet material with a working field level of ≈1 T in a working volume of $0.5 \times 0.25 \times 0.02$ m^3 were used for the first time in the construction of this accelerator. The electron energy increment per a single

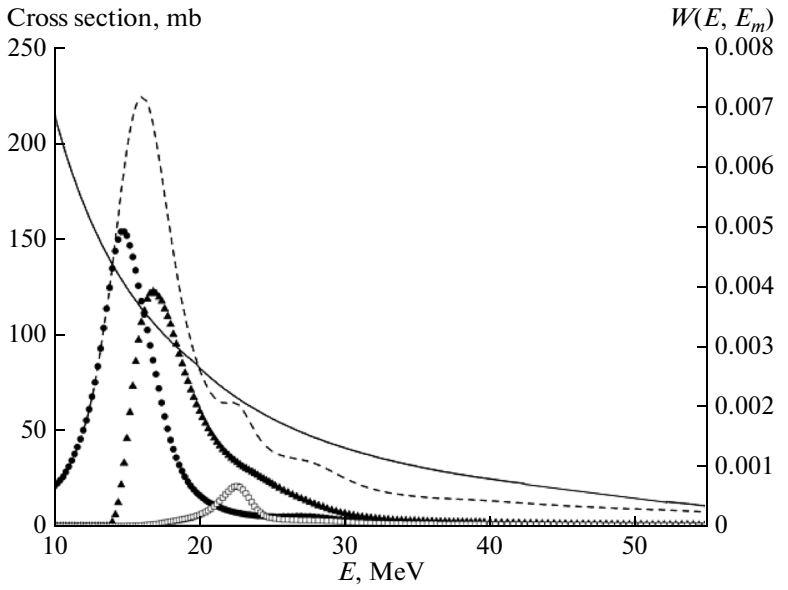

Fig. 2. Bremsstrahlung spectrum $W(E, E_m)$ of gamma quanta for a maximum electron energy of 67.7 MeV (solid line). The theoretically calculated cross section $\sigma = \sigma(\gamma, n) + \sigma(\gamma, p) + \sigma(\gamma, 2n)$ of a reaction on the ^{100}Mo molybdenum isotope is shown with a dashed line. Partial cross sections $\sigma(\gamma, n)$, $\sigma(\gamma, p)$, and $\sigma(\gamma, 2n)$ are indicated with circles (●), squares (▲), and triangles (□), respectively.

beam revolution was roughly equal to 5 MeV. The electron energy at the accelerator output may be varied by altering the number of revolutions within a range of 14.9–67.7 MeV. The pulse current of an extracted electron beam reached 40 mA and the pulse length equaled 2–20 μs.

The experiment was carried out at the maximum electron beam energy of 67.7 MeV. The extracted electron beam was incident on a 2.5-mm-thick wolfram target in which the bremsstrahlung gamma radiation concentrated in the direction of propagation of the initial electron beam was produced (Fig. 1). In order to reconstruct the shape of the bremsstrahlung γ-quanta spectrum, the interaction of an electron beam with an energy of 67.7 MeV with a 2.5-mm-thick wolfram target was modeled on a computer using the GEANT-4 software package. The obtained energy dependence of the γ-quanta spectrum was then smoothed and approximated with a smooth function. This function was used in calculations of the theoretical yields of photonuclear reactions.

Figure 2 shows the bremsstrahlung γ-radiation spectrum for our experiment calculated for a single accelerator electron. Theoretically calculated cross sections of various photonuclear reactions on the ^{100}Mo molybdenum isotope are also shown.

The residual activity spectra were measured with a coaxial ultrapure germanium detector (Canberra, GC3019) with an efficiency of 30%. The energy resolution of the detector equaled 0.9 and 1.9 keV for the energies of 122 keV and 1.33 MeV, respectively. The detector was installed in a special room located about 30 meters away from the accelerator hall. This made it possible to measure the residual activity spectra of the sample several minutes after the irradiation. The detector was fitted with lead and copper shielding, which considerably improved the background conditions of the measurements and allowed us to detect rare cases of radioactive isotope production in multiple photonuclear reactions.

A 0.3-mm-thick square (2.5 × 2.5 cm) metal plate made from a natural mixture of molybdenum isotopes (with the following isotopic composition: 9.82% of ^{100}Mo, 24.39% of ^{98}Mo, 9.60% of ^{97}Mo, 16.67% of ^{96}Mo, 15.84% of ^{95}Mo, 9.15% of ^{94}Mo, and 14.53% of ^{92}Mo) was used as a target in the present study. The target was irradiated with a beam of bremsstrahlung photons with a maximum energy of 67.7 MeV for 4 h and 25 min. Under such conditions, γ-activity from photonuclear reactions with the ejection of one or several neutrons and protons was produced in the target. The measurements of the induced activity spectra began 8 min after the irradiation. A total of 331 series of spectra of varying durations (from 90 s to 30 min) were measured. The total duration of measurements of the spectra amounted to 6 days.

The search for the γ-quanta spectra maxima and the calculation of their intensities were conducted using an automated system of spectra measurement and analysis [13]. The automated spectra measurement and analysis software allows one to visualize the data, resolve overlapping peaks, and approximate them with Gaussian curves using the least-squares method and standard algorithms. About 100 maxima

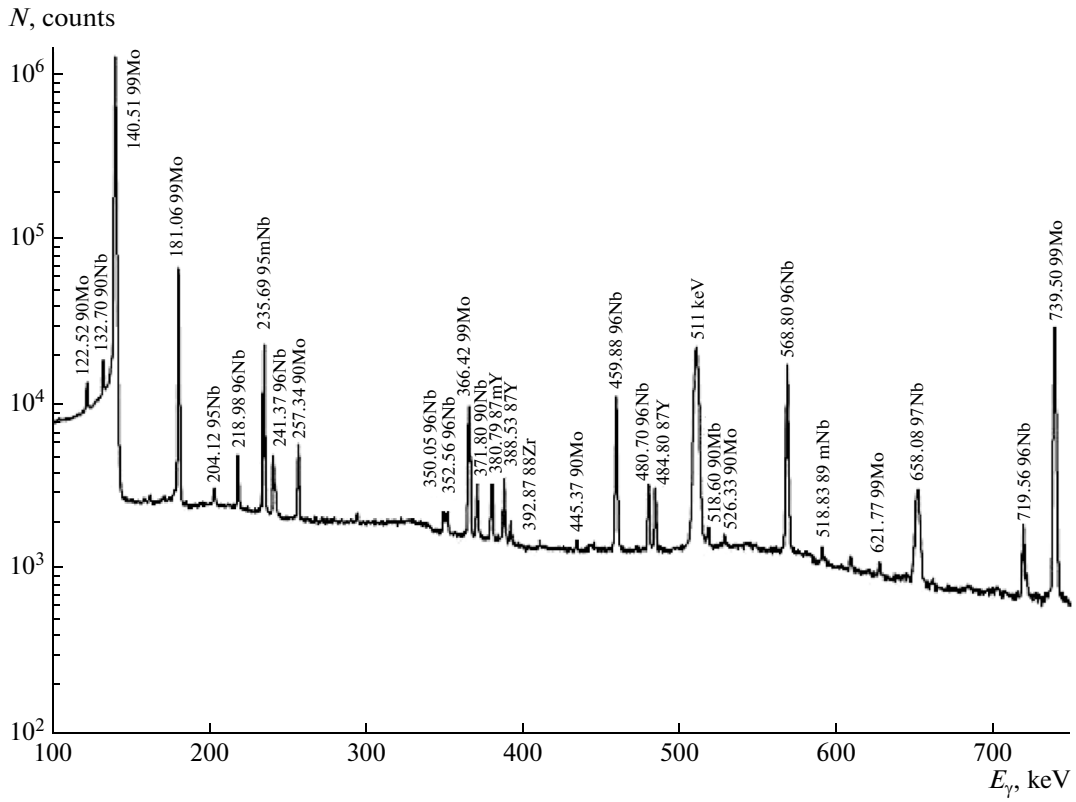

Fig. 3. Gamma quanta spectrum in an energy range of 100–750 keV from the target made from a natural mixture of molybdenum isotopes irradiated with a bremsstrahlung spectrum with an upper limit at 67.7 MeV.

corresponding to the production of various radioactive isotopes within the irradiated target were found in the γ-quanta spectra. Figure 3 shows one of the measured γ-spectra with certain of the most intense peaks labeled according to their nature. A large number of peaks, which correspond to the decay of the formed β-radioactive nuclei into various states of the end nuclei are observed in the spectrum. The peak energies and the end beta-radioactive nuclei of the photonucleon reaction that lead to the emergence of each peak are indicated. For example, β-radioactive isotopes ^{90}Mo and ^{96}Nb are formed in reactions ^{92}Mo(γ, $2n$)^{90}Mo and ^{97}Mo(γ, p)^{96}Nb, respectively.

Let us show how the data on a photonuclear reaction were extracted using the γ-activation technique through the example of the ^{92}Mo(γ, $2n$)^{90}Mo reaction (Fig. 4). The (γ, $2n$) reaction, as well as any other photonuclear reaction on a medium or heavy nucleus, proceeds over a characteristic time of $\approx 10^{-19}$ s. The end nucleus (^{90}Mo) may end up in both the ground and the excited states. The excitation is usually relaxed by emitting electric dipole (E1), electric quadrupole (E2), or magnetic dipole (M1) gamma quanta over a time interval of 10^{-9}–10^{-17} s (de-excitation quanta are not detected by the γ-spectrometer). After this, the ^{90}Mo nucleus (in its ground state by then) undergoes β^+-decay or electron capture. This decay results in various states of the ^{90}Nb end nucleus and is characterized by a half life $t_{1/2} = 5.56$ h. The gamma quanta spectrum detected by the germanium spectrometer will contain a set of the corresponding γ-lines characteristic of ^{90}Nb. Thus, the detected γ-quanta spectrum shows that precisely the (γ, $2n$) reaction in $^{92}_{42}$Mo took place. The peaks in the spectrum are identified based on the energy of γ-transitions and the half-life time. The energy of β-decay of the formed isotopes is usually large and reaches several megaelectronvolts. As a result, a large number (up to 20) of γ-transitions in daughter nuclei correspond to the decays of these isotopes. The correctness of identification of a certain reaction may also be verified by comparing its yields calculated based on different γ-peaks: if the reaction is identified correctly, these yields should be equal.

If a radioactive isotope may be formed only as a direct result of the photonuclear reaction, the corresponding yield was calculated using the following formula:

$$Y = \frac{S\lambda}{k(e^{-\lambda(t_2-t_1)} - e^{-\lambda(t_3-t_1)})(1-e^{-\lambda t_1})}, \qquad (1)$$

where S is the photopeak area gained over the measurement time, t_1 is the irradiation time, t_2 is the measurement start time, t_3 is the measurement end time,

λ is the decay constant, and k is a coefficient equal to a product of the detector efficiency, the cascade summing coefficient, and the quantum yield of γ-quanta at γ-transitions.

However, the studied isotopes may be formed not only as a direct result of photonuclear reactions, but also as a result of accumulation in the process of decay of parent nuclei formed in the photonuclear reaction. For example, the ^{90}Nb niobium isotope may be formed both as a direct result of the ^{92}Mo(γ, pn)^{90}Nb reaction and in the consequent β-decay of the ^{90}Mo isotope (^{90}Mo $\xrightarrow{\varepsilon}$ ^{90}Nb) formed as a result of the ^{92}Mo(γ, $2n$)^{90}Mo reaction. The photonuclear reactions may in certain cases produce end nuclei not only in the ground state, but also in the isomeric (after de-excitation) state. Therefore, the contributions of isomeric states were taken into account in the calculations of the overall reaction yield. Specifically, an isomeric niobium isotope state ^{95m}Nb that is formed as a result of the ^{96}Mo(γ, p)^{95m}Nb reaction decays into the ground niobium isotope state ^{95}Nb in 94% of the cases, while in only 5.6% of the cases it undergoes β^+-decay. Systems of differential equations describing the radioactive decay sequence while accounting for the branching ratios for different decay channels were solved in order to determine the isotope yields in such cases.

2. EXPERIMENTAL RESULTS

The reactions observed in our experiment, the corresponding end nuclei with their spins and parities, the decay types and half-lives, the reaction thresholds and yields, and the results of theoretical calculations are listed in the table.

The reaction yields presented in the table were determined using the following relationship:

$$Y(E_m) = n\int_{E_{\text{th}}}^{E_m}\sigma(E)W(E, E_m)dE, \qquad (2)$$

where n is the number of studied irradiated nuclei, $\sigma(E)$ is the energy-dependent reaction cross-section, E_{th} is the reaction threshold, and $W(E, E_m)$ is the spectrum of bremsstrahlung radiation photons with an upper limit E_m (i.e., the number of photons with energy E in the unit energy interval in the spectrum of bremsstrahlung photons produced in unit time by monochromatic electrons with a kinetic energy $E_e = E_m$). The spectrum of bremsstrahlung photons $W(E, E_m)$ with $E_m = 67.7$ MeV is shown in Fig. 2.

Index m in the isotope mass number indicates that this isotope is formed in an isomeric (long-lived) excited state, ε indicates β^+-decay or electron capture, and IT (isomeric transition) indicates that the isomeric state decays through the ejection of a gamma quantum or an internal conversion electron.

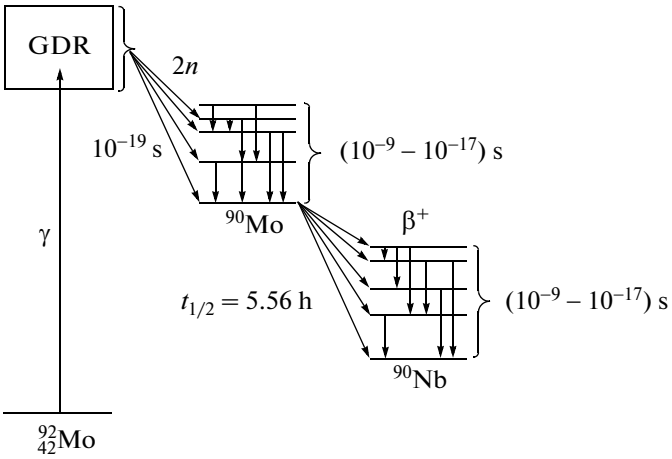

Fig. 4. Development of the ^{92}Mo(γ, $2n$)^{90}Mo reaction.

The experimental and theoretical yields are normalized to the ^{100}Mo(γ, n)^{99}Mo reaction yield that was taken to be equal to 100. The ^{99}Mo end nucleus could also be formed as a result of the ^{100}Mo(γ, p)^{99}Nb reaction with a consequent β^--decay (^{99}Nb $\xrightarrow{\beta^-}$ ^{99}Mo), but the contribution of this reaction to the production ^{99}Mo did not exceed the experimental error.

The rightmost column of the table lists the results of a theoretical calculation of the measured yields. The experimental results are compared to these calculated data with the use of a theoretical model [5], which is briefly described in the next section.

Unresolved experimental yields of a sum of two reactions leading to the production of one and the same end nucleus were obtained in four cases. The ratio between the yields of these competing reaction channels was estimated in two cases (^{97}Mo(γ, p) + ^{98}Mo(γ, pn) and ^{96}Mo(γ, p) + ^{97}Mo(γ, pn)) within the framework of the theoretical model and is indicated in the rightmost column of the table opposite the reactions.

3. THEORETICAL MODEL

The photonucleon reactions were described theoretically using CMPR [5]. In accordance with Bohr's assumption, this model splits the reaction into two independent stages: the formation of an excited state of a nucleus and its decay into reaction products. The first stage of the reaction is described using the semimicroscopic vibration model (SVM) [14, 15] and the quasideuteron photoabsorption model (QPM) [16, 17], and the second one is described using the exciton model (EM) [18] and the evaporation model (EvM) [19].

The processes of photoabsorption with the excitation of the isovector giant dipole resonance that is prevalent in the $E_\gamma < 40$ MeV energy region and is basi-

The characteristics of the reactions on molybdenum isotopes observed for bremsstrahlung photons with an upper limit at 67.7 MeV

Reaction	End nucleus and its spin-parity	$t_{1/2}$ and the decay type of the end nucleus	Threshold, MeV	Experimental reaction yield (experimental error)	Theory	
^{100}Mo(γ, *n*)	^{99}Mo($1/2^+$)	66.98 h (β^-)	8.29	100 (6)	100	
^{100}Mo(γ, *pn*)	^{98m}Nb(5^+)	51.3 min (β^-)	18.10	0.309 (0.028)		
^{98}Mo(γ, *p*)	^{97}Nb($9/2^+$)	72.1 min (β^-)	9.79	6.62 (0.05)	7.8	
^{97}Mo(γ, *p*) ^{98}Mo(γ, *pn*)	^{96}Nb(6^+)	2.35 h (β^-)	9.23 17.87	11.04 (0.82)	10.1	7.7 2.7
^{96}Mo(γ, *p*) ^{97}Mo(γ, *pn*)	^{95}Nb($9/2^+$)	34.99 days (β^-)	9.30 16.72	14.14 (0.43)	15.0	10.0 (γ, *p*)
^{96}Mo(γ, *p*) ^{97}Mo(γ, *pn*)	^{95m}Nb($1/2^-$)	3.61 days (IT + β^-)	9.53 16.95			5.0 (γ, *pn*)
^{94}Mo(γ, *pn*) ^{94}Mo(γ, *pn*)	^{92}Nb(7^+) ^{92m}Nb(2^+)	3.47×10^7 years (ε) 10.15 days (ε)	17.32 17.45	2.56 (0.02)	3.0	
^{92}Mo(γ, *n*)	^{91}Mo($9/2^+$)	15.49 min (ε)	12.68	33.5 (4.2)	65	
^{92}Mo(γ, 2*n*)	^{90}Mo(0^+)	5.56 h (ε)	22.78	5.08 (0.40)	2.7	
^{92}Mo(γ, *pn*)	^{90}Nb(8^+)	14.60 h (ε)	19.51	14.0 (4.5)	3.5	
^{92}Mo(γ, *p*2*n*) ^{92}Mo(γ, 3*n*)^{89}Mo $\xrightarrow{\varepsilon}$ ^{89}Nb	^{89}Nb($9/2^+$)	2.03 h (ε)	29.59	1.91 (0.21)	0.85	
^{92}Mo(γ, *p*2*n*) ^{92}Mo(γ, 3*n*)^{89}Mo $\xrightarrow{\varepsilon}$ ^{89m}Nb	^{89m}Nb($1/2^-$)	66 min (ε)	29.62	1.77 (0.27)		
^{92}Mo(γ, 4*n*)	^{88}Mo(0^+)	8 min (ε)	46.39	0.046 (0.006)	0.006	

cally a coherent mix of one-particle–one-hole ($1p1h$) excitations are described within the framework of SVM. The isovector giant quadrupole resonance (GQR) plays a significant role at energies above the GDR energy. The GQR contribution is also taken into account in the calculations.

A simple semimicroscopic model in which the main groups of one-particle transitions are considered to be degenerate (and the residual interaction is approximated with multipole–multipole forces) is used in the SVM. The energies and integral cross sections of the main GDR and GQR peaks and the isospin GDR splitting were calculated within the framework of this approach. The GDR width was estimated using a semiempirical formula from [20] and the GQR width was determined using the exciton model [18].

The mechanism of interaction between photons and nuclei is altered at $E_\gamma > 40$ MeV. In contrast to the giant-dipole resonance region where photons interact with a nucleus as an undivided object, a photon in the region above this resonance interacts (due to the wavelength reduction and kinematic constraints related to the conservation of momentum) with systems comprise a small number of nucleons within the nucleus and, first and foremost, with quasideuterons (bound proton–neutron clusters). Thus, two photodisintegration mechanisms (the traditional one that acts through the excitation of giant dipole resonance and the nonresonance, quasideuteron (QD) type) compete with each other. This process is described in CMPR using a QPM version developed by Chadwick [17] and taking the influence of the Pauli blocking effect on the cross sections of QD absorption into account.

In the considered theoretical approach, the process of photonucleon emission from medium and heavy nuclei is divided into two stages: the pre-equilibrium one and the evaporative one. In order to take these two stages into account, the probability densities for the formation of states with various numbers of excitons in the intermediate nucleus and the probability density for achieving thermal equilibrium in this nucleus are calculated in CMPR. The probability densities are calculated using recurrent relationships that tie them to the probabilities of the formation of exciton and equilibrium states at the earlier stages of decay. These densities are used to calculate the cross sections of var-

ious photonucleon reactions and isolate the contributions of pre-equilibrium and evaporative processes.

An important feature of CMPR distinguishing it from the TALYS [21] model that is frequently used in similar calculations consists in the fact that CMPR takes into account the isospin structure of GDR, without which it is not possible to describe correctly the relation between the probabilities of GDR decay with the emission of protons and neutrons. This is achieved through a corresponding modification of the densities of exciton and total states of the end nucleus.

Figure 5 showcases the capabilities of CMPR that is used to describe the main channels of photoneutron disintegration of the ^{100}Mo isotope the (γ, n) cross section of which is used for normalizing the measured yields. The theoretical calculation data shown in Fig. 5 are compared with the results of an experiment in which ^{100}Mo was irradiated with quasimonochromatic photons and subjected to photoneutron disintegration [8]. The giant dipole resonance that decays predominantly into the (γ, n) and (γ, $2n$) channels is prevalent at energies below 25 MeV. The contributions of these channels in the 25–40 MeV energy region are relatively small. It follows from Fig. 5 that CMPR reproduces both the shapes and the values of experimental cross sections well. Therefore, this model may be used as a sufficiently reliable theoretical basis for the analysis of experimental results on the nuclear photodisintegration of molybdenum isotopes.

4. DISCUSSION

The table gives a comparison between the experimental data and the results of theoretical calculations carried out using CMPR. A good agreement between the experiment and the theory is observed for four (^{98}Mo(γ, p), ^{97}Mo(γ, p) + ^{98}Mo(γ, pn), ^{96}Mo(γ, p) + ^{97}Mo(γ, pn), and ^{94}Mo(γ, pn)) out of eight reactions with the largest measured yields. A significant discrepancy between the experiment and the theory is observed for the other four reactions (^{92}Mo(γ, n), ^{92}Mo(γ, pn), ^{92}Mo(γ, $2n$), and ^{92}Mo(γ, $p2n$) + ^{92}Mo(γ, $3n$)) all of which involve the least heavy molybdenum isotope ^{92}Mo. For example, a twofold reduction in the yield relative to the theoretically calculated yield of the most intense photoneutron reaction ^{92}Mo(γ, n) is observed. The experimental yield of the second-most intense reaction (γ, pn) observed for ^{92}Mo is several times greater than the theoretical estimate. In order to reveal the possible reasons for the mentioned discrepancies between the experiment and the theory, we shall look closer at the other molybdenum isotopes.

Figure 6 shows the yields of photonuclear reactions for all molybdenum isotopes with mass numbers ranging from 89 to 103. These yields were calculated within the framework of CMPR using the experimental bremsstrahlung radiation spectrum. The yields of the most probable photonucleon reactions ((γ, n), (γ, $2n$), and (γ, p)) and the total yields of all reactions on each isotope γ, $abs = \gamma$, $n + \gamma$, $2n + \gamma$, $p + ...$ are shown. Both the theoretical and the experimental yields were normalized to the ^{100}Mo(γ, n) reaction yield, which was taken to be equal to 100.

The (γ, n) reaction is the prevalent one for molybdenum isotopes with $A \geq 93$. According to both the experimental data [7, 8] and the CMPR calculation results, this reaction dominates for all molybdenum isotopes in this mass region and forms 55–77% of the total (all the GDR decay channels included) yield. The (γ, n) reaction yield for the considered isotopes remains roughly at the same level (100–110 in the chosen system of units), while the (γ, $2n$) reaction yield increases with increasing mass number from 3.5 (for ^{93}Mo) to 50–70 (for ^{102,103}Mo). Such diverse behaviors of the yields of reactions (γ, n) and (γ, $2n$) in the region of $A = 93$–103 may be attributed to the thresholds of these reactions. The (γ, n) reaction thresholds remain roughly at the same level as A increases: they vary from 5.4 to 8.1 MeV for odd isotopes and from 8.1 to 9.7 MeV for even isotopes. The (γ, $2n$) reaction thresholds, on the other hand, are decreased markedly (from 22.8 MeV for ^{93}Mo to 13.5 MeV for ^{103}Mo) with increasing A. This results in a significant increase in the average neutron energy and the penetration of the centrifugal barrier for neutrons and leads to a corresponding increase in the probability of emission of a pair of neutrons.

The total yield of all reactions (γ, *abs*) is noticeably increased in the transition from light molybdenum isotopes to heavier ones. It can be seen from Fig. 6 that this increase is explained by an increase in the (γ, $2n$) reaction yield.

As for the (γ, p) reaction, its yield is small (up to 10% on average) in comparison to the total photoneutron yield for isotopes with $A = 93$–103 and is systematically increased with decreasing A from 2.4 for ^{103}Mo to 14.9 for ^{93}Mo. This correlates with the corresponding systematic decrease in the photoproton threshold from 11.8 MeV (^{103}Mo) to 7.6 MeV (^{93}Mo). This decrease results in an increase in the penetration of the centrifugal barrier for protons in the transitions from heavy molybdenum isotopes to lighter ones.

As the mass number is reduced to $A = 92$, the proton yield is increased sharply: according to the theoretical calculations, its share in the total yield reaches 40%. As A is reduced further to 90–89, the share of the proton yield in the total yield exceeds 50%. The sharp increase in the proton yield at $A = 92$ and lower mass numbers is accompanied by a corresponding reduction in the yield of the (γ, n) reaction that ceases to be the prevalent one at $A = 89$–90 and gives way the (γ, p) reaction.

The theoretically predicted effect of a sharp increase in the (γ, p) reaction yield at $A = 92$ and the corresponding decrease in the (γ, n) reaction yield is confirmed by the data gathered in our experiment.

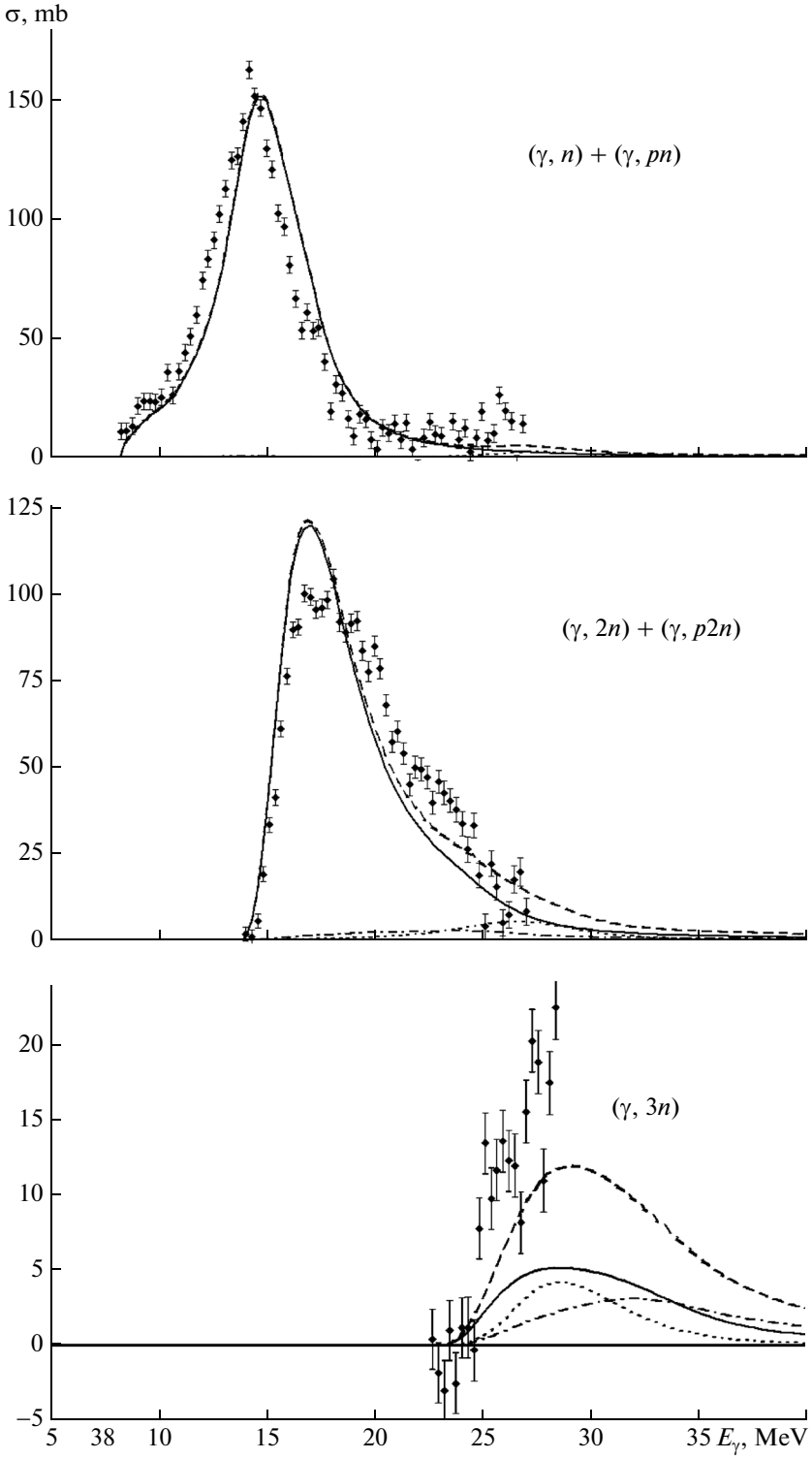

Fig. 5. Cross sections of the main photoneutron reactions for the ^{100}Mo nucleus. Points with error bars correspond to the experimental data from [8]. Lines denote the results of CMPR calculations: dashed lines indicate total cross-sections, solid lines trace the GDR contribution, dotted lines correspond to the quadrupole resonance, and dash-and-dot lines correspond to the quasi-deuteron reaction mechanism.

According to the data presented in the table, the total observed yield of the reaction for ^{92}Mo with neutrons in the end state amounts to 50–60, or 40–50% of the total yield (125–130) predicted theoretically. The difference between the total and the observed yields should be attributed primarily to the ^{92}Mo(γ, p)^{91}Nb

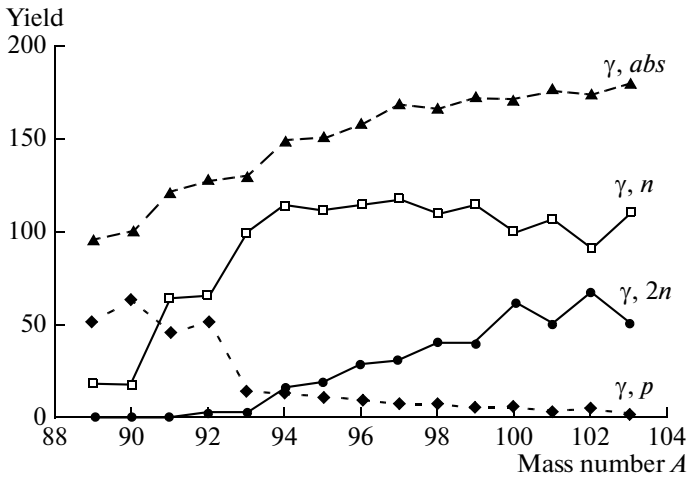

Fig. 6. Relative yields of the main photonucleon reactions an the total yields of all reactions (γ, *abs*) for molybdenum isotopes with mass numbers A ranging from 89 to 103. The yields are calculated within the framework of the combined model of photonucleon reactions with a bremsstrahlung photon spectrum with an upper limit at 67.7 MeV. The ^{100}Mo(γ, n) reaction yield is taken to be equal to 100.

reaction that could not be observed in our experiment due to the half life of the end nucleus $^{91}\text{Nb} \xrightarrow{\varepsilon} {}^{91}\text{Zr}$ being too large (680 years). A relatively low (33.5) value of the observed yield of the ^{92}Mo(γ, n) reaction is also indicative of a significantly enhanced role of the ^{92}Mo(γ, p) reaction.

The results of experiment [9] also lead to the conclusion that the photoproton GDR decay channel plays an important role in ^{92}Mo. The authors of [9] obtained an integral cross section of about 700 MeV mb in an excitation energy range of 14.4–25.4 MeV for the ^{92}Mo[(γ, p) + (γ, pn) + 2(γ, p)] reaction. This cross section amounts to about 50% of the classical dipole sum rule ($60\frac{NZ}{A}$ MeV mb).

The main reason for a sharp increase in the photoproton yield in light molybdenum isotopes downwards from ^{92}Mo lies in their shell structure. These isotopes are proton-excess isotopes and are located on the boundary of the β-stability band. The considered light isotopes also differ from the other (heavier) molybdenum isotopes in that the system of their one-particle neutron levels ends with level $1g_{9/2}$, which closes the $1f2p1g_{9/2}$ outer shell. The outer neutrons of all the other molybdenum isotopes with nucleon numbers ranging from 93 to 103 start to fill one-particle levels of the next shell ($1g_{7/2}2d3s1h_{11/2}$) that is separated from the $1f2p1g_{9/2}$ shell by an energy gap of 3–4 MeV. This results in the fact that the neutron separation energy for light molybdenum isotopes (it equals 12.67 MeV for ^{92}Mo) is 3–6 MeV higher than the corresponding energy for other stable molybdenum isotopes. Thus, the proton Fermi surface in ^{92}Mo and lighter molybdenum isotopes is, contrary to the other molybdenum isotopes, located about 5 MeV higher than the neutron Fermi surface. Therefore, the average energies of emitted neutrons in ^{92}Mo and lighter isotopes are significantly lower than the average proton energy. Consequently, the neutron penetration and yield are reduced considerably and the relative proton yield in light molybdenum isotopes downwards from ^{92}Mo is increased.

The cause of the almost threefold increase in the ^{92}Mo(γ, pn) reaction yield relative to the theoretical one requires additional study. It may also turn out to be the consequence of the discussed high probability of proton emission from a ^{92}Mo nucleus excited to GDR energies. If the end ^{91}Nb nucleus has a considerable probability of being placed in states with excitation energies in excess of the neutron-separation energy as a result of such emissions, the probability of their consequent ejection may turn out to be rather large.

CONCLUSIONS

Novel experimental data on the yields of various photonuclear reactions for the molybdenum isotopes ^{92,94,96,97,98,100}Mo were obtained using the γ-activation technique in the region of γ-quanta energies of up to 67.7 MeV. These data were analyzed together with the results of calculating the photodisintegration of all (including the unstable ones) molybdenum isotopes with $A = 89$–103 within the framework of CMPR. In general, this model gives a decent description of the experimental data. A sharp increase in the photoproton yield and the corresponding decrease in the photoneutron yield were observed for ^{92}Mo and lighter isotopes. This effect was interpreted based on the shell structure of molybdenum isotopes.

REFERENCES

1. B. S. Ishkhanov and I. M. Kapitonov, *Interaction of Electromagnetic Radiation with Atomic Nuclei* (Moscow, 1979) [in Russian].
2. M. Danos, B. S. Ishkhanov, N. P. Yudin, and R. A. Eramzhyan, Phys.-Usp. **38**, 1297 (1995).
3. B. S. Ishkhanov, N. P. Yudin, and R. A. Eramzhyan, Fizika Element. Chastits At. Yadra **31**, 313 (2000).
4. B. S. Ishkhanov and I. M. Kapitonov, *Giant Dipole Resonance of Atomic Nuclei* (Moscow, 2008) [in Russian].
5. B. S. Ishkhanov and V. N. Orlin, Phys. At. Nucl. **74**, 19 (2011).
6. N. Mutsuro, Y. Ohnuki, K. Sato, and M. Kimura, J. Phys. Soc. Jpn. **14**, 1649 (1959).
7. B. S. Ishkhanov, I. M. Kapitonov, E. V. Lazutin, et al., Yader. Fizika **11**, 702 (1970).
8. H. Beil, R. Bergere, P. Carlos, et al., Nucl. Phys. A **227**, 427 (1974).
9. K. Shoda, H. Miyase, M. Sugawara, et al., Nucl. Phys. A **239**, 397 (1975).
10. V. V. Varlamov, N. E. Stepanov, and V. V. Chesnokov, Izv. Akad. Nauk, Ser. Fiz. **67**, 656 (2003).
11. I. Boboshin, V. V. Varlamov, D. Rudenko, and M. Stepanov, Vopr. At. Nauki Tekhn., Ser. Yader. Konst. **2**, 99 (1999).
12. R. Firestone and L. Ekstrom, Table of Radioactive Isotopes **1**, 1 (1999).
13. M. B. Chadwick, M. Herman, P. Oblozinsky, et al., Nucl. Data Sheets **112**, 2887 (2011).
14. V. I. Shvedunov, A. N. Ermakov, I. V. Gribov, et al., Nucl. instruments and methods, Physics Res. Sect. A. Accelerators, Spectrometers, Detectors and Associated Equipment **550**, 39 (2005).
15. S. S. Belyshev, A. A. Kuznetsov, A. S. Kurilik, and K. A. Stopani, *58-e mezhdunar. soveshchanie po yader. spektroskopii i strukture atomnogo yadra "Yadro-2008". Problemy fundamental'noi yadernoi fiziki. Razrabotka yaderno-fizicheskikh metodov dlya nanotekhnologii, meditsinskoi fiziki i yadernoi energetiki": Tezisy Dokl* (Proc. 58th Int. Meeting on Nuclear Spectroscopy and Atomic Nucleus Structure "Nucleus-2008". Problems of Fundamental Nuclear Physics. Development of Nuclear-Physical Methods for Nanotechnology, Medical Physics and Nuclear Energetics) 2008.
16. B. S. Ishkhanov and V. N. Orlin, Phys. Part. Nucl. **38**, 232 (2007).
17. B. S. Ishkhanov and V. N. Orlin, Phys. At. Nucl. **76**, 30 (2013).
18. J. S. Levinger, Phys. Rev. **84**, 43 (1951).
19. M. B. Chadwick, P. Obloinsky, P. E. Hodgson, and G. Reffo, Phys. Rev. C: Nucl. Phys. **44**, 814 (1991).
20. C. K. Cline and M. Blann, Nucl. Phys. A **172**, 225 (1971).
21. J. M. Blat and V. F. Vaiskopf, *Theoretical Nuclear Physics* (New York, 1952).
22. B. S. Ishkhanov and V. N. Orlin, Phys. At. Nucl. **66**, 659 (2003).
23. A. J. Koning, S. Hilaire, and M. C. Duijvestijn, *Proc. Int. Conf. on Nuclear Data for Science and Nechnology* Nice, France, 2007.
24. A. J. Koning and J. P. Delaroche, Nucl. Phys. A **713**, 231 (2003).

Translated by D. Safin